Journal Pre-proof

3D-printed polymer foams maintain stiffness and energy dissipation under repeated loading

Younghoon Kwon, Soyoung E. Seo, Jaejun Lee, Szabolcs Berezvai, Javier Read de Alaniz, Claus D. Eisenbach, Robert M. McMeeking, Craig J. Hawker, Megan T. Valentine

PII: S2452-2139(22)00395-3

DOI: https://doi.org/10.1016/j.coco.2022.101453

Reference: COCO 101453

To appear in: *Composites Communications*

Received Date: 31 August 2022

Revised Date: 16 November 2022

Accepted Date: 8 December 2022

Please cite this article as: Y. Kwon, S.E. Seo, J. Lee, S. Berezvai, J. Read de Alaniz, C.D. Eisenbach, R.M. McMeeking, C.J. Hawker, M.T. Valentine, 3D-printed polymer foams maintain stiffness and energy dissipation under repeated loading, *Composites Communications* (2023), doi: https://doi.org/10.1016/j.coco.2022.101453.

Credit author statement

Kwon: Conceptualization, Methodology, Software, Formal Analysis, Investigation, Data Curation, Writing - Original Draft, Visualization.

Seo: Methodology, Resources, Writing – Review & Editing.

Lee: Methodology, Writing – Review & Editing.

Berezvai: Methodology, Formal Analysis, Writing – Review & Editing.

Read de Alaniz: Supervision, Writing – Review & Editing.

Eisenbach: Investigation, Writing – Review & Editing.

McMeeking: Methodology, Supervision, Writing – Review & Editing.

Hawker: Methodology, Resources, Supervision, Writing – Review & Editing.

Valentine: Conceptualization, Methodology, Resources, Data Curation, Visualization, Writing - Original Draft, Supervision, Project Administration, Funding Acquisition.

3D-printed polymer foams maintain stiffness and energy dissipation under repeated loading

Younghoon Kwon [a,b], Soyoung E. Seo [c], Jaejun Lee [d], Szabolcs Berezvai [e], Javier Read de Alaniz [b,f], Claus D. Eisenbach [b,g], Robert M. McMeeking [a,b,h,i,j], Craig J. Hawker [b,f,h], Megan T. Valentine [a,b,*]

[a] Department of Mechanical Engineering, University of California Santa Barbara
[b] Materials Research Laboratory, University of California Santa Barbara
[c] School for Engineering of Matter, Transport and Energy, Arizona State University
[d] Department of Polymer Science and Engineering, Pusan National University, Busan 46241, Republic of Korea
[e] Department of Applied Mechanics, Budapest University of Technology and Economics
[f] Department of Chemistry and Biochemistry, University of California Santa Barbara
[g] Institute for Polymer Chemistry, University of Stuttgart, 70569 Stuttgart, Germany
[h] Materials Department, University of California Santa Barbara
[i] School of Engineering, Aberdeen University, King's College, Aberdeen AB24 3UE, Scotland
[j] INM – Leibniz Institute for New Materials, Campus D2 2, 66123 Saarbrücken, Germany

[*] Correspondence: valentine@engineering.ucsb.edu

Abstract

Additive manufacturing enables the fabrication of bio-inspired materials possessing intricate architectures across broad length scales leading to systems that are simultaneously stiff, tough, and lightweight. A digital light processing (DLP) strategy was used to additively manufacture polymer foams with controlled porosity through the incorporation of thermally expandable microspheres. Following initial photopolymerization, a subsequent thermal processing step reproducibly allows access to a broad range of foam densities. Using uniaxial compression, we investigated how foaming impacts the mechanics of the composite material, including modulus, Poisson's ratio, and energy dissipation. It was observed that the 3D-printed foams are remarkably resilient under cyclic loading, with sustained values of both modulus and energy dissipation under repeated loading at large deformations.

Keywords

DLP 3D-printing, polymer foam, compression, resilience, energy absorptive

1. Introduction

Natural composites have long inspired the design and fabrication of advanced functional materials. Cellular structures (*e.g.*, foams) such as bone and wood maintain high mechanical stiffness despite their low density [1]. Their hierarchical porosity provides myriad mechanisms for deformation and toughening, and spatial heterogeneities (*i.e.*, soft and hard phases) and porosity gradients provide effective paths to mitigate stress concentrations and dissipate energy [2, 3]. Despite the performance advantages imparted by these natural design motifs, manufacturing bio-inspired materials with control over multiscale feature has been challenging due to inherent limitations of conventional manufacturing methods [4]. The advent of additive manufacturing has improved capabilities for the on-demand fabrication of complex three-dimensional (3D) objects [3, 5] with digital light processing (DLP) of photocurable resins being a versatile and promising approach for the production of porous and hierarchical materials at high speed and resolution [6-8].

We recently developed a two-step DLP-based 3D printing approach that exploits an initial photopolymerization step followed by the thermal expansion of embedded microspheres. By controlling the initial microsphere weight fraction, closed-cell composite polymer foams with variable porosity and tunable mechanical properties are obtained [9]. Here, we report material processing methods that improve reproducibility with detailed mechanical analysis of the compressive behaviors of the foams illustrating unique energy dissipation and fatigue performance. These thermally-activated 3D-printed foams are remarkably resilient under high strain cyclic loading, maintaining energy dissipation capability and stiffness. Our results establish that 3D-printed polymer foams are good candidates for use as lightweight, energy-absorbing materials.

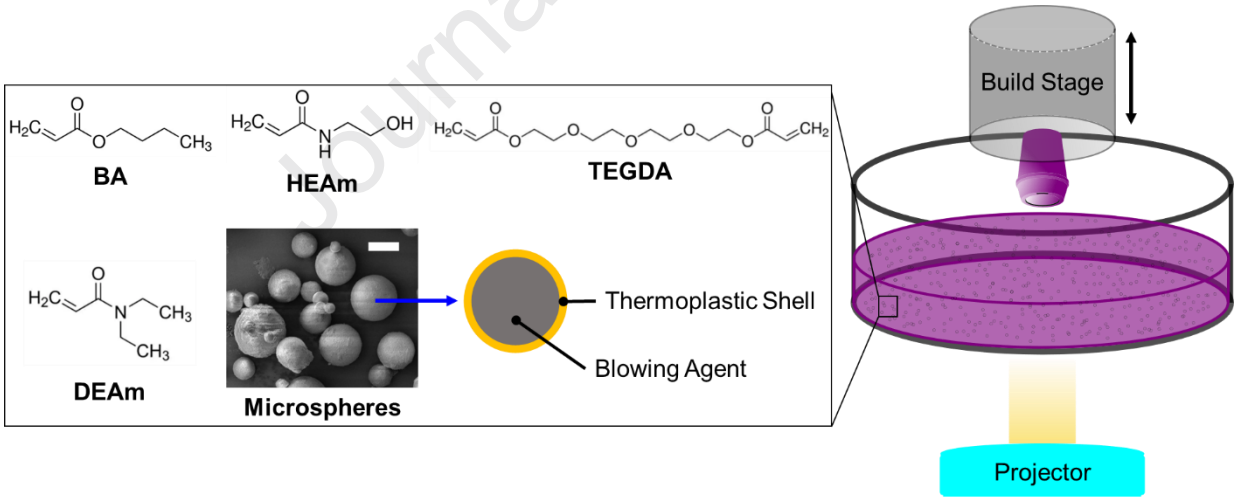

Figure 1. Schematics of the DLP printing set up. The resin mixture contains monomers (butyl acrylate (BA); *N*, *N*-diethyl acrylamide (DEAm); *N*-hydroxyethyl acrylamide (HEAm)), cross-linker (tetra ethylene glycol diacrylate (TEGDA), photochemicals, and microspheres that are filled with a volatile hydrocarbon core. The thermoplastic shell is an acrylonitrile-MMA copolymer. Scale bar, 10μm. The homogenized resin mixture is photopolymerized in a layer-by-layer fashion under exposure to visible light.

2. Materials and Methods

2.1. Material Preparation

The formulated resin for 3D-printing includes a combination of monomers (butyl acrylate (BA); *N*, *N*-diethyl acrylamide (DEAm); *N*-hydroxyethyl acrylamide (HEAm)), cross-linker (tetra ethylene glycol diacrylate (TEGDA)), photosensitizers (Sudan IV; Sudan black B), accelerators (H-Nu 254; Borate V), and initiator (Erythrosine B) with different loading fractions of microspheres (Expancel 051DU40, Nouryon) added as foaming agents, (Resin formulation 1) [9]. Each thermally-expandable microsphere comprises a volatile hydrocarbon core encased in a thermoplastic shell. Mean diameters of the microspheres before and after thermal expansion were measured to be 9.4±2.5 μm and 25.0±9.7 μm, respectively (Fig. S1). All monomers were filtered through a plug of basic alumina to remove inhibitors and stabilizers. The resin mixture was introduced to a glass vial with septum and was sonicated to homogenize and uniformly disperse the microspheres throughout the network, which ensures isotropic volumetric expansion upon foaming. Care was taken to minimize unwanted photopolymerization by covering the formulated resin foil with minimal light exposure during fabrication.

2.2. 3D-photopolymerization and Thermal Processing

A custom-built printing vat, compatible with an FEP film (0.001", Teflon) as the release layer, was employed for printing (Fig. S2). Briefly, prior to printing, the septum-sealed vat and vial containing the resin were sparged with argon for 10 minutes. The resin was transferred to the vat using an argon-purged syringe. The vat was placed over the light source (5040UB, Epson projector) which provided a digital image (*i.e.*, 2D cross-section of 3D object) and the printing stage, which could be immersed in the resin, was positioned near the FEP film-resin interface using a linear translation stage. Photopolymerization was performed under a flow of argon, layer by layer, until the desired 3D object was completed. Exposure time and layer thickness were determined as described [9]. After printing, parts were removed from the stage using a razor blade, washed with isopropanol, dried and heated at 70 ℃ for ~24 hours to drive the polymerization reaction to completion. To induce pore formation, the cured samples were then heated for 15 min at 110 ℃, which is above the activation temperature for the embedded microspheres. During this second thermal treatment, the thermoplastic shells soften, and the evaporation and expansion of the hydrocarbon generates vapor pressure in the core. This leads to sphere expansion and formation of closed-cell foam morphologies within the continuous photopolymer matrix.

3. Results and Discussion

We previously demonstrated that the combination of DLP 3D printing and thermal processing allows fabrication of thermally-activated polymer foams [9]. However, we observed batch-to-batch variation in print quality and occasionally obtained malformed printed samples. To improve reproducibility, several modifications to the initial synthetic protocol were made. First, FEP films were employed in lieu of fluorinated oil, which we found could cause undesirable air bubbles to be trapped in printed layers as the moving stage was repeatedly immersed in the resin mixture. The use of FEP eliminated such defects, which compromised mechanical performance, and produced more reliable parts.

In addition, we modified the cure schedule and introduced a heating step at 70 °C for ~24 hours to fully cure the photopolymerized network and avoid any network curing during the thermal microsphere expansion step. In the absence of this modification, unwanted network curing can occur during expansion of the microspheres, leading to abnormally high variations in stiffness (Fig. S3-S4) [10]. To avoid this, we post-cured the as-printed samples at a higher temperature (70 °C) for a longer period (24 hours) and then immediately performed the thermal treatment (110 °C) for activation of microsphere expansion (Fig. S5). The resultant foam is a porous composite consisting of a continuous rubbery matrix into which glassy polymer shells are embedded. These modifications, which made no changes to the material chemistry, imparted significant improvements in reproducibility, while still providing broad control over the level of porosity. Interestingly, the formation of macroscale core-shell pattern was observed in the printed cylindrical samples (Fig. S6). Scanning electron microscopy (SEM) imaging revealed an inner core containing large (100~200μm) and small pores (~25μm) surrounded by an outer zone containing only small pores near the surface of the 3D-printed object. We speculate that these radial differences arise due to the trapping of the evaporated hydrocarbon gas in the core, which in turn promoted pore coalescence and the formation of large pores. By contrast, the gas can more readily diffuse out of the 3D-printed object near the surface, leading to smaller pore sizes at the surface. This radial gradient is not explicitly considered in the mechanical analysis that follows, but this effect could be leveraged in future structural designs.

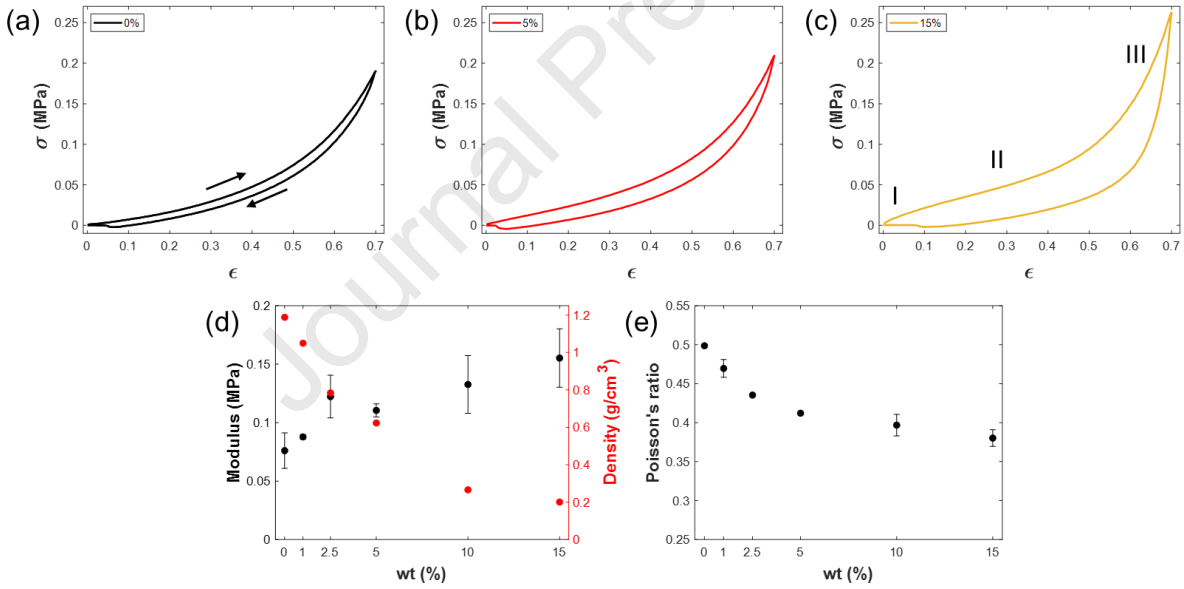

Figure 2. Stress-strain curves from the uniaxial compression tests. (a) Unfilled polymer matrix shows non-linear elastic behavior and small hysteresis upon unloading. On the contrary, the composite foams at (b) 5% and (c) 15% microsphere fraction showed three distinct regions (see panel c), and significant energy dissipation was observed (data for other microsphere weight fractions are shown in Fig. S7). (d) The measured elastic compression modulus increases, and density decreases as a function of microsphere weight fraction which increases porosity. (e) The Poisson's ratio also decreases with increasing porosity.

The mechanical properties of six different weight fractions (*wt*%) of microspheres were investigated, ranging from 0% (i.e., polymer matrix only with no porosity) to 15 *wt*% of microspheres. Uniaxial compression of cylindrical samples was performed as described [9]. A maximum strain of 70% was applied to each sample, which was then unloaded to zero displacement at strain rate of $0.001\mathrm{s}^{-1}$. Sample surfaces

were lubricated (high vacuum grease, Dow Corning) to minimize barreling. The pure unfilled matrix (0%) followed the non-linear stress-strain relationship (Fig. 2a), typical of elastomers [11]. In contrast, polymer foams show three distinct regions of response (Fig. 2b-c), consistent with prior measurements of syntactic foams [12].

At the smallest strains (ε = 0.005 to 0.1), a linear region was observed, due to the stiffness of the shell walls and continuous matrix forming the composite material. The measured Young's modulus increased with increasing microsphere fraction (Fig. 2d and Fig. S7d). We attribute this to the increased contribution of the shell walls which are glassy at room temperature, with modulus of ~44 MPa, significantly exceeding that of the polymer matrix (~76 kPa) (Fig. S8). Although the continuous matrix is critical to loading bearing [13], the shell contributions to stiffness outweigh the reduction of the matrix volume as density decreases upon microsphere addition, leading to the observed increase in composite modulus upon foaming. As a result, the specific modulus increased by more than an order of magnitude from 64 to 773.5 kPa $(\mathrm{g\ cm^{-3}})^{-1}$ (Fig. S7) when the microsphere fraction increased from 0% to 15%. At intermediate strains, a softening plateau was observed, which we attribute to the onset of shell buckling that reduces the measured stress; this contrasts the response of glass-based syntactic foams where a strong yield plateau is observed due to the irreversible breakage of the glass shells. At even higher compressive strains, a third regime emerges. Here, the samples stiffened, due to the densification of highly compacted microspheres that allows the sample to withstand higher stresses in the large deformation regime. Divergence of the nonlinear mechanical behaviors as a function of microsphere fraction is more pronounced when the data are plotted using a variant of Mooney plot (Fig. S9) where the stress is normalized by measured modulus and presented as a function of stretch. The constitutive relation is based on the Neo-Hookean hyperelastic model which accurately describes the mechanical response of rubber-like materials [14]. We observed a monotonic deviation from simple Neo-Hookean response (which would give a linear relation on the Mooney plot) as the *wt%* increased, indicating an important role for the glassy polymeric shells in determining the overall mechanical response of the composite. The Poisson's ratio (υ) was also measured using image analysis of recorded time-lapse videos during mechanical tests (Fig. S10). As porosity increased, υ decreased (Fig. 2e) from nearly 0.5 for the incompressible pure matrix to a value of ~ 0.38 for 15% microsphere fraction due to the increased void volume in the porous samples.

Next, we probed the response of pristine samples to incremental cyclic loading using a Texture Analyzer (TA.XTPlus Connect, Texture Technologies) with a 50N load cell at a crosshead speed of 0.01 mm/s. Strain was programmed to increase gradually from 15% to 70% (Fig. S11a). At each strain level, 3 cycles of loading and unloading were collected. In all cases, we found hysteresis between the loading and unloading curves, indicating dissipated energy during the cycle, which became more prominent at high microsphere weight fraction (Fig. 4a). We attribute this dissipation to shell buckling, as observed using scanning electron microscopy (Fig. S13). Interestingly, the re-loading curves largely followed the initial loading weight fraction, rather than the path of the previous unloading curves and the extent of hysteresis was fairly robust over 3 cycles of recurrent strain (Fig. 3d-f), suggesting the elastic recovery of microspheres from shell buckling.

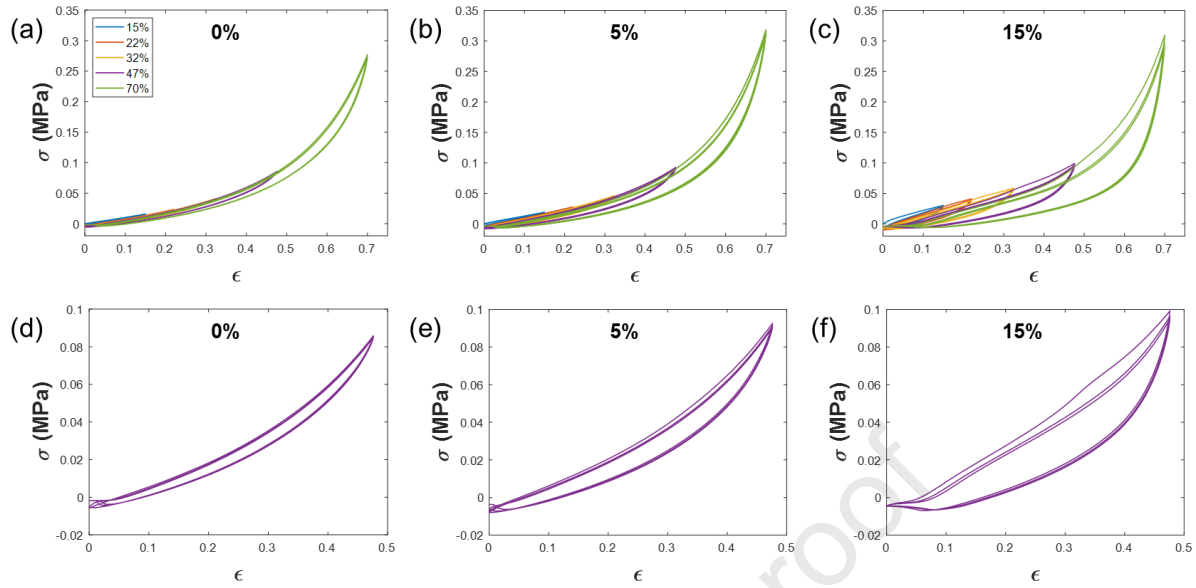

Figure 3. (a)-(c) Stress-strain curves from incremental cyclic loading for three representative microsphere fractions (data from other weight fractions are shown in Fig. S11). At each strain level (indicated by color) 3 measurements were performed. (d)-(f) 3 cycles at 47% strain highlighting the extent of elastic recovery upon unloading, as well as the increase in energy dissipation for higher microsphere fractions.

To further examine their resilience, the printed materials were subjected to fatigue testing using 100 cycles of 70% strain at 0.01 mm/s, the slowest available crosshead speed to approximate quasistatic loading (Fig. 4b). For the pure polymer matrix (0%), we saw almost no decrease in dissipated energy as a function of cycle number. For composite foams, particularly at 10-15 *wt*% of microparticles, we observed an initial decrease in dissipated energy of about 30-40% for the first few cycles. This reduction was associated with stress softening, where a smaller stress is needed at the equivalent strain level on subsequent loading cycles (Fig. S12). We speculate that this is due to the slow recovery of the microspheres. We observed that stress softening diminishes as the number of cycles increases possibly due to the development of plastic deformation, leading to non-zero strain at zero stress after 100 cycles for samples prepared from 10-15 *wt*%.

It was particularly noteworthy that despite this plastic deformation, the composites retain a significantly higher capability for energy dissipation as compared to the pure matrix under large deformation. And after a drop in energy dissipation over the first 3-5 cycles, the values stabilized and no significant changes in the energy dissipation properties were observed for up to 100 cycles total. Moreover, the modulus was sustained throughout the 100 cycles (Fig. 4c), even when significant plastic deformation of the polymer shells had been observed (Fig. S13). Similar recovery was observed using conventional methods to generate all-polymer composite foams using polymeric microspheres in a continuous polyurethane matrix, in contrast to the response of syntactic foams formed using hollow glass spheres that tend to fracture, rather than buckle, and thus show poor recoverability and resilience [11]. Future studies will examine the effect of increasing the loading rate, to better understand possible viscoelastic effects and possibly to enable fatigue analysis of larger cycle numbers in experimentally accessible timescales.

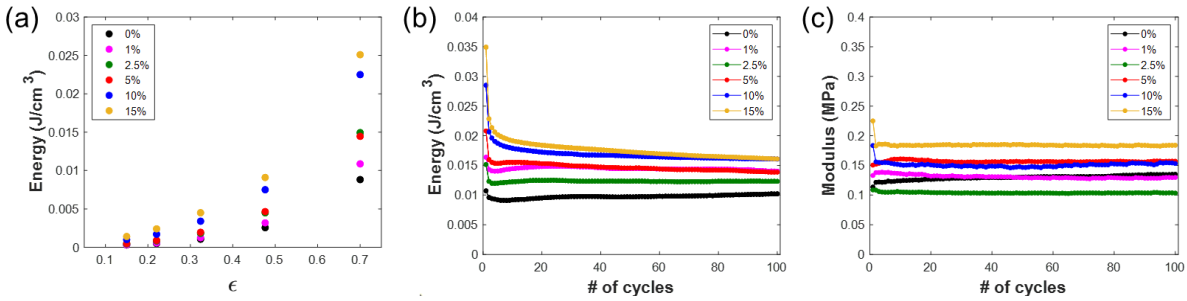

Figure 4. (a) Dissipated energy (*i.e.*, the area of the hysteresis loop as shown in Figure 3) during incremental cyclic testing. Data points represent the mean value of 3 cycles at each strain level. (b) Energy dissipation and (c) elastic modulus over 100 cycles.

4. Conclusions

We generated robust porosity-controlled polymer foams using a two-step process of DLP 3D printing followed by the expansion of thermally-activated microspheres. A significant increase in specific modulus, which we attribute to high modulus disparity between the matrix and glassy polymeric shell of the compacted microspheres, was observed. As porosity increased, the density and Poisson's ratio decreased while energy dissipation under cyclic loading increased. The printed foams were observed to be remarkably fatigue tolerant, retaining superior energy dissipation capabilities and stiffness under repeated loading even into the moderate to large strain regime where microscopic plastic deformation was discerned. These results demonstrate the potential of these additively manufactured composite foams for applications ranging from construction, packaging and cushioning while also laying the foundation for future mechanical modeling and material design using polymeric building blocks.

Credit author statement

Kwon: Conceptualization, Methodology, Software, Formal Analysis, Investigation, Data Curation, Writing - Original Draft, Visualization. **Seo:** Methodology, Resources, Writing – Review & Editing. **Lee:** Methodology, Writing – Review & Editing. **Berezvai:** Methodology, Formal Analysis, Writing – Review & Editing. **Read de Alaniz:** Supervision, Writing – Review & Editing. **Eisenbach:** Investigation, Writing – Review & Editing. **McMeeking:** Methodology, Supervision, Writing – Review & Editing. **Hawker:** Methodology, Resources, Supervision, Writing – Review & Editing. **Valentine:** Conceptualization, Methodology, Resources, Data Curation, Visualization, Writing - Original Draft, Supervision, Project Administration, Funding Acquisition.

Acknowledgements

This work was supported by the MRSEC Program of the National Science Foundation (NSF) under Award No. DMR 1720256 (IRG-3). SES and CJH acknowledge support by the U.S. Army Research Office under Cooperative Agreement W911NF-19-2-0026 for the Institute for Collaborative Biotechnologies. This research was supported by the Hungarian National Research, Development and Innovation Office (Grant no. NKFI-PD 137806). The authors acknowledge the use of the Microfluidics Laboratory within the California NanoSystems Institute, supported by the University of California, Santa Barbara and the University of California, Office of the President and Mechanical Test Lab of the UCSB Mechanical Engineering Department, and leveraged resources provided by NSF Award No. DMR 1933487. Authors

appreciate useful discussions with Christopher Barney, Juan Manuel Urueña, David Bothman and Kirk Fields.

Declaration of competing interest: No interests to declare.

References

[1] Wegst UG, Bai H, Saiz E, Tomsia AP, Ritchie RO. Bioinspired structural materials. Nature materials. 2015;14(1):23-36.
[2] Liu Z, Meyers MA, Zhang Z, Ritchie RO. Functional gradients and heterogeneities in biological materials: Design principles, functions, and bioinspired applications. Progress in Materials Science. 2017;88:467-98.
[3] Truby RL, Lewis JA. Printing soft matter in three dimensions. Nature. 2016;540(7633):371-8.
[4] Mirzaali M, De La Nava AH, Gunashekar D, Nouri-Goushki M, Veeger R, Grossman Q, et al. Mechanics of bioinspired functionally graded soft-hard composites made by multi-material 3D printing. Composite Structures. 2020;237:111867.
[5] Schaedler TA, Carter WB. Architected cellular materials. Annual Review of Materials Research. 2016;46:187-210.
[6] Kuang X, Wu J, Chen K, Zhao Z, Ding Z, Hu F, et al. Grayscale digital light processing 3D printing for highly functionally graded materials. Science advances. 2019;5(5):eaav5790.
[7] Meza LR, Zelhofer AJ, Clarke N, Mateos AJ, Kochmann DM, Greer JR. Resilient 3D hierarchical architected metamaterials. Proceedings of the National Academy of Sciences. 2015;112(37):11502-7.
[8] Moore DG, Barbera L, Masania K, Studart AR. Three-dimensional printing of multicomponent glasses using phase-separating resins. Nature materials. 2020;19(2):212-7.
[9] Seo SE, Kwon Y, Dolinski ND, Sample CS, Self JL, Bates CM, et al. Three-dimensional photochemical printing of thermally activated polymer foams. ACS Applied Polymer Materials. 2021;3(10):4984-91.
[10] Kloosterboer J, Lijten G. Chain cross-linking photopolymerization of tetraethyleneglycol diacrylate: thermal and mechanical analysis. ACS Publications; 1988.
[11] Yousaf Z, Smith M, Potluri P, Parnell W. Compression properties of polymeric syntactic foam composites under cyclic loading. Composites Part B: Engineering. 2020;186:107764.
[12] Doman D, Cronin D, Salisbury C. Characterization of polyurethane rubber at high deformation rates. Experimental Mechanics. 2006;46(3):367-76.
[13] Wouterson EM, Boey FY, Hu X, Wong S-C. Specific properties and fracture toughness of syntactic foam: Effect of foam microstructures. Composites science and technology. 2005;65(11-12):1840-50.
[14] Brown R. Physical testing of rubber: Springer Science & Business Media; 2006.

Highlights

- Resilient, lightweight polymer foams with controlled porosity are 3D-printed
- Two-step processing allows access to a broad range of foam densities
- Modulus, Poisson's ratio, and energy dissipation of the composite are measured
- 3D-printed foams are remarkably resilient under cyclic loading, even at high strain

Declaration of interests

☒ The authors declare that they have no known competing financial interests or personal relationships that could have appeared to influence the work reported in this paper.

☐ The authors declare the following financial interests/personal relationships which may be considered as potential competing interests: